Variation of Ionic Strength Reveals the Interfacial Water Structure at a Charged Mineral Surface

Kailash C. Jena and Dennis K. Hore*

Department of Chemistry, University of Victoria, Victoria, British Columbia, V8W 3V6, Canada

Received: June 11, 2009

We have used visible-infrared sum-frequency generation spectroscopy to study the structure of water molecules that form the interface with fused silica. Spectra throughout the OH-stretching region were collected in two different polarization schemes so that the orientation of interfacial water molecules could be studied. A depth profiling experiment was performed by varying the ionic strength, thereby peeling away the outskirts of this interfacial region, leaving water molecules progressively closer to the charged interface. As the ionic strength increases, the spectral intensity drops since the interfacial region is becoming thinner. However, we notice a change in the relative contribution of tetrahedrally coordinated molecules compared to those that make less hydrogen bonds. We have the opportunity to study these two water species individually; we conclude that the higher coordination species exists some distance away from the interface and is oriented close to the plane of the surface with a mean tilt angle ~70° and a narrow tilt and twist distribution. We have evidence that lower coordination water molecules are close to the interface and offer two possibilities for their orientation that are consistent with our data. One has a twist angle distribution centered in the plane of the interface, tilted ~35° from the normal. The other possibility is that they are twisted out of the plane of the interface and tilted ~30° from the normal. As the electrolyte concentration increases, we observe a reduction of the mean tilt angle in all cases. This is consistent with a picture of molecules nearer to the surface better aligned in the presence of a stronger interfacial field.

SEOK, SANGJUN
04/17/2010

Experimental section

Laser : mode-locked Nd:YAG 30 ps laser, 10 Hz

Sample cell was fabricated from Teflon and clamped IR-grade fused silica prism

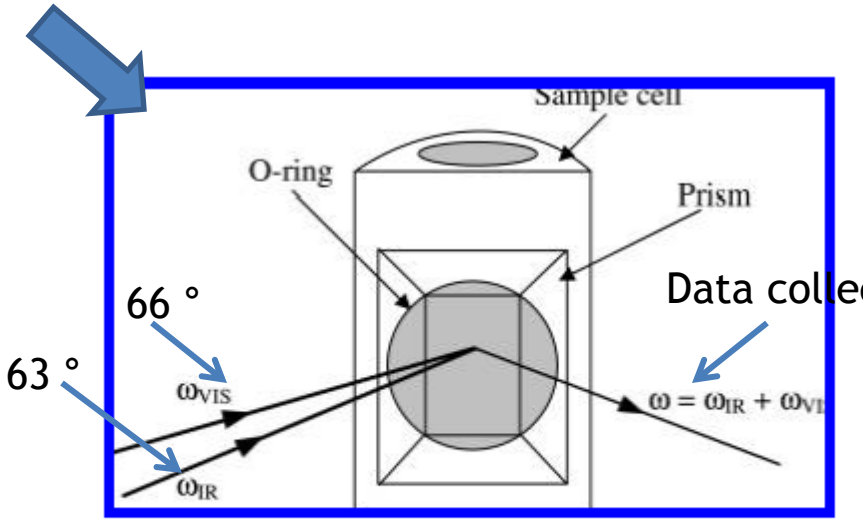

Data collection averaged 50 shots

Figure 1. Schematic diagram of the sample cell compartment. Infrared and visible beams are overlapped at the prism-water interface at the back side of the prism.

Pure water was used for the experiments and to prepare the NaCl solutions.

Spectra were acquired under two polarization schemes denoted by SSP and SPS.

Results

1. Pure Water-Fused Silica Interface and Ionic Strength Studies

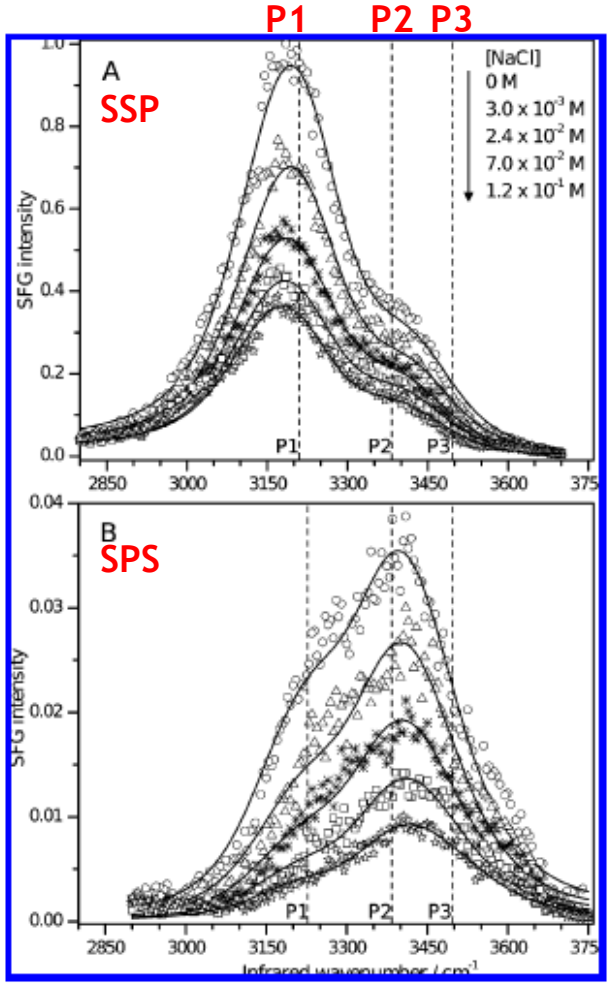

Figure 2. Sum−frequency spectra of interfacial water structure in the presence of varying NaCl concentration at the fused silica surface, collected in (a) ssp and (b) sps polarizations, after correcting for local field effects. The spectra shown are therefore directly proportional to (a) $|\chi^{(2)}_{yyz}|^2$ and (b) $|\chi^{(2)}_{yzy}|^2$. Quantitative comparisons may be made since the intensity axes have been normalized with repect to the ssp signal from the fused silica−water interface. Intensity decreases monotonically as NaCl concentration increases.

BLE 1: Fitting Parameters for the Spectra Displayed in Figure 2

Polarization	[NaCl]/10^{-3} M	A_1/au	A_2/au	A_3/au	R^2 fit
ssp	0.000	7.68 ± 0.50	3.25 ± 0.21	−0.076 ± 0.005	0.991
	3.4 ± 0.1	6.46 ± 0.41	2.86 ± 0.18	−0.066 ± 0.004	0.990
	24 ± 1	5.60 ± 0.32	2.65 ± 0.15	−0.057 ± 0.003	0.992
	70 ± 2	4.99 ± 0.37	2.49 ± 0.18	−0.051 ± 0.004	0.986
	120 ± 4	4.57 ± 0.40	2.32 ± 0.20	−0.047 ± 0.004	0.981
sps	0.000	1.23 ± 0.12	1.74 ± 0.17	0.18 ± 0.02	0.974
	3.4 ± 0.1	0.89 ± 0.11	1.50 ± 0.15	0.19 ± 0.02	0.962
	24 ± 1	0.67 ± 0.08	1.27 ± 0.16	0.19 ± 0.02	0.960
	70 ± 2	0.56 ± 0.08	1.15 ± 0.16	0.22 ± 0.03	0.956
	120 ± 4	0.45 ± 0.07	0.89 ± 0.13	0.26 ± 0.04	0.928

P1 : icelike as “tetrahedral” (symmetric stretching)

P2 : liquidlike

P3 : antisymmetric

SSP : P1 has a larger amplitude than P2 while for SPS P1<P2

Water species may very well be different.

Results

1. Pure Water-Fused Silica Interface and Ionic Strength Studies

P1/P2 ratio disordered as the ionic strength increases.

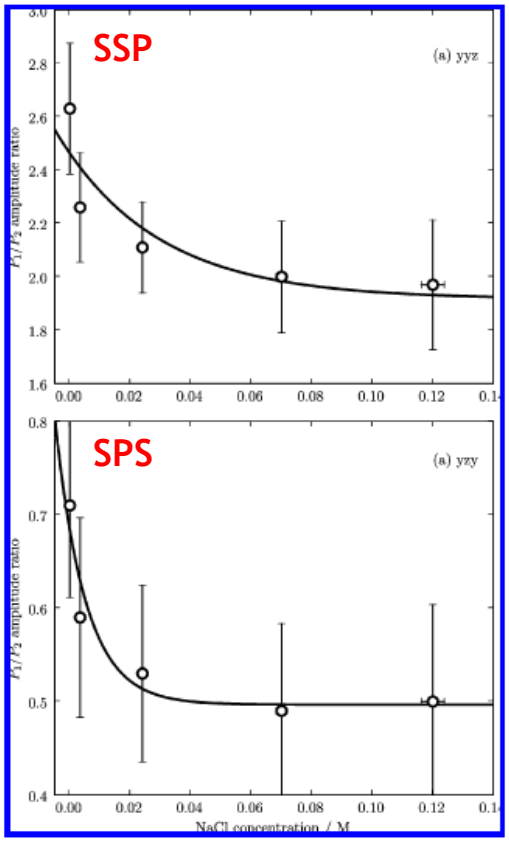

Figure 3. Amplitude ratio P_1/P_2 for (a) $\chi^{(2)}_{yyz}$ and (b) $\chi^{(2)}_{yzy}$.

C_{2v} symmetry assumption

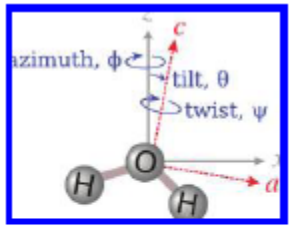

Figure 4. This figure illustrates the convention that we use to describe the Cartesian coordinates (*a*, *b*, *c*) in the molecular frame and (*x*, *y*, *z*) in the lab frame. For simplicity, this is illustrated with the molecular *b*-axis aligned with the lab *y*-axis, both directed into the page. The water molecule is in the *ac*-plane with *c* parallel to its C_2 rotation axis. The tilt angle θ is the angle between the surface normal *z* and the molecular *c*-axis. The twist angle ψ describes rotation about the molecular *c*-axis.

Water symmetric stretch nonvanishing elements : α_{aac}, α_{bbc} and α_{ccc}

Water antisymmetric stretch nonvanishing elements : $\alpha_{aca} = \alpha_{caa}$

Projecting the molecular elements into the yyz(yzy) lab. frame

$$\alpha^{(2),ss}_{yyz} = \frac{1}{2}\cos\theta[\alpha^{(2)}_{ccc} + \alpha^{(2)}_{aac} + (\alpha^{(2)}_{bbc} - \alpha^{(2)}_{aac})\cos^2\psi] - \frac{1}{2}\cos^3\theta[\alpha^{(2)}_{ccc} - \alpha^{(2)}_{bbc} + (\alpha^{(2)}_{bbc} - \alpha^{(2)}_{aac})\cos^2\psi]$$

$$\alpha^{(2),ss}_{yzy} = \frac{1}{2}\cos\theta[\alpha^{(2)}_{ccc} - \alpha^{(2)}_{bbc} + (\alpha^{(2)}_{bbc} - \alpha^{(2)}_{aac})\cos^2\psi] - \frac{1}{2}\cos^3\theta[\alpha^{(2)}_{ccc} - \alpha^{(2)}_{bbc} + (\alpha^{(2)}_{bbc} - \alpha^{(2)}_{aac})\cos^2\psi]$$

$$\alpha^{(2),as}_{yyz} = \cos\theta(-\alpha^{(2)}_{aca}\cos^2\psi) + \cos^3\theta(\alpha^{(2)}_{aca}\cos^2\psi)$$

$$\alpha^{(2),as}_{yzy} = \frac{1}{2}\cos\theta(\alpha^{(2)}_{aca} - 2\alpha^{(2)}_{aca}\cos^2\psi) + \cos^3\theta(\alpha^{(2)}_{aca}\cos^2\psi)$$

For each of the above expressions, we then consider

$$\chi^{(2)}_{ijk} = \frac{N}{\varepsilon_0}\langle\alpha^{(2)}_{ijk}\rangle = \frac{N}{\varepsilon_0}\frac{\int_0^{2\pi}\int_0^{\pi} f_{ODF}\alpha^{(2)}_{ijk}\sin\theta\,d\theta\,d\psi}{\int_0^{2\pi}\int_0^{\pi} f_{ODF}\sin\theta\,d\theta\,d\psi}$$

Orientation Distribution Function (ODF)

Mean tilt angle Mean twist angle

$$f_{ODF} = \exp\left[-\frac{(\theta-\theta_0)^2}{2\sigma_\theta^2} - \frac{(\psi-\psi_0)^2}{2\sigma_\psi^2}\right] \qquad \sigma_\psi = a\cos^2\theta_0$$

Results

1. Pure Water-Fused Silica Interface and Ionic Strength Studies

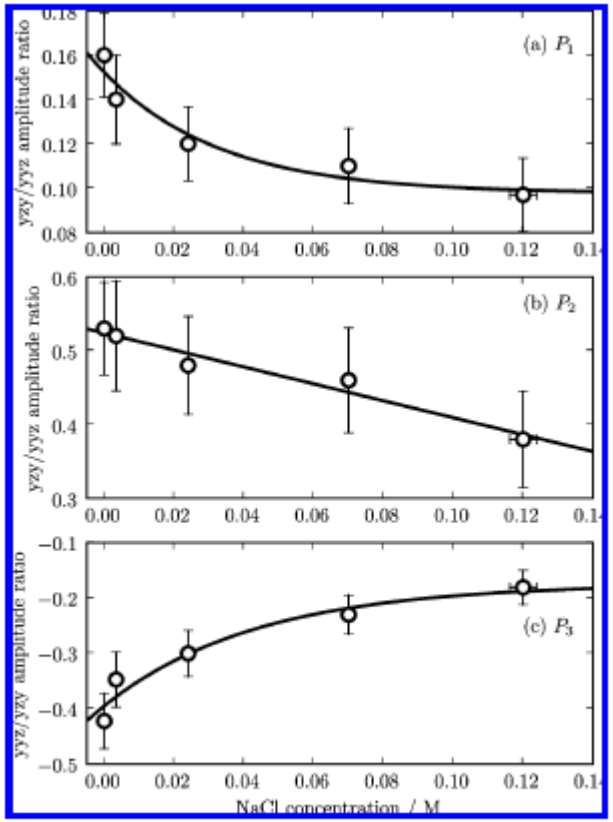

Figure 5. Ratio of the water-fused silica yzy/yyz ampltudes for (a) P_1 and (b) P_2 as the ionic strength of the solution is increased. Panel (c) shows the yyz/yzy amplitude ratio for P_3.

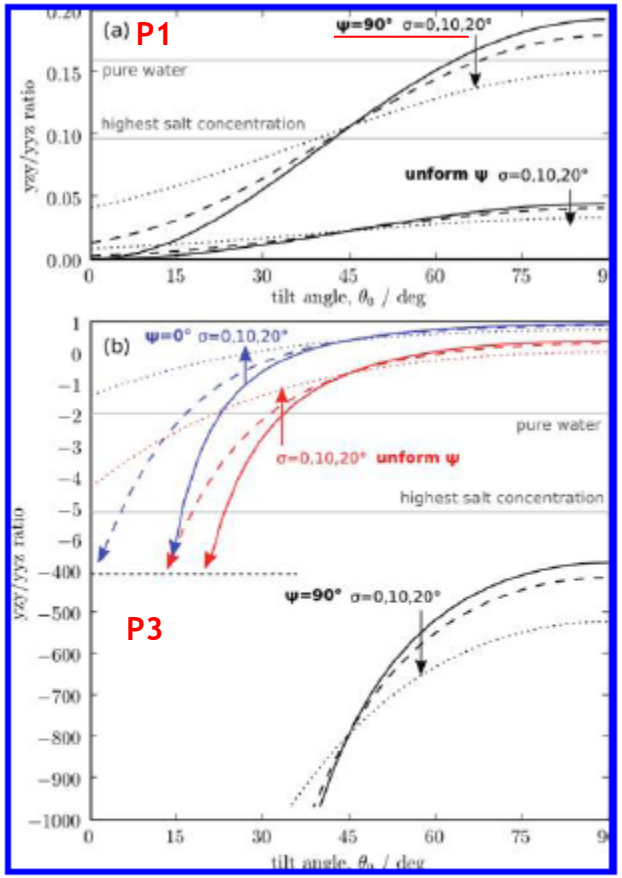

Figure 6. (a) Ratio of yzy/yyz amplitudes as a function of the mean tilt angle θ_0 for water symmetric stretch (P_1). The top three curves illustrate the case of a narrow distribution of twist angles $\delta(\psi - 90°)$ for three possible tilt distributions, narrow $\delta(\theta - \theta_0)$, Gaussian with $\sigma_\theta = 10°$, and $\sigma_\theta = 20°$. Also shown is the case of infinite wide (uniform) distribution of twist angles for the same three tilt distributions. (b) The same cases are illustrated for the antisymmetric band P_3. In addition, here we consider one additional set of curves illustrating a narrow twist distribution about $\psi_0 = 0°$.

Results

2. Water Orientation at the Fused Silica Surface

Case 1: Both Water Species Lie in the Plane of the Interface.

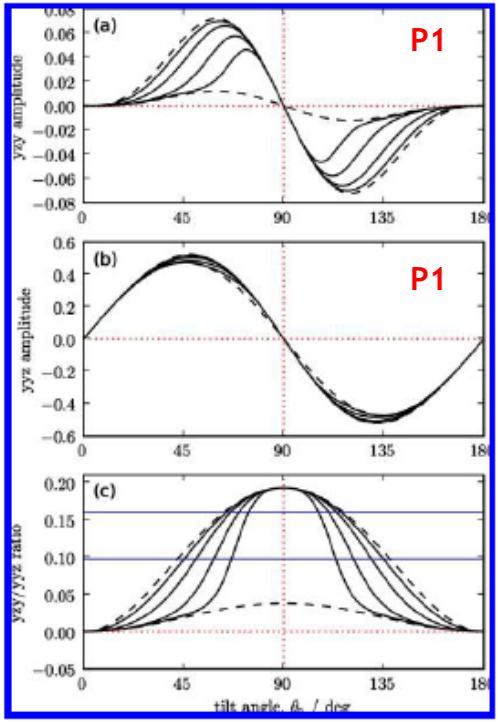

Figure 7. Prediction of (a) A_{yzy} and (b) A_{yyz} amplitude as a function of the mean tilt angle for the P_1 population symmetric stretch with our hybrid orientation distribution function. Here, in the narrow limit, the twist angle is centered at 90° when the water molecules are constrained by large tilt angles. For comparison, the limiting cases of wide/uniform and fixed twist angles are shown with dashed lines. (c) The A_{yzy}/A_{yyz} ratio. Limiting cases for experimental values are indicated by the horizontal solid lines.

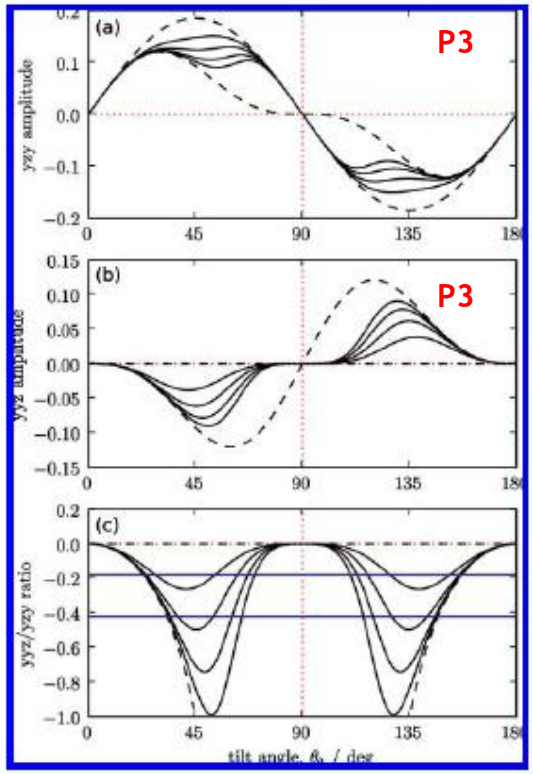

Figure 8. Prediction of (a) A_{yzy} and (b) A_{yyz} amplitude as a function of the mean tilt angle for the P_3 population antisymmetric stretch with our hybrid orientation distribution function. Here, in the narrow limit, the twist angle is centered at 90° when the water molecules are constrained by large tilt angles. For comparison, the limiting cases of wide/uniform and fixed twist angles are shown with dashed lines. (c) The A_{yyz}/A_{yzy} ratio. Limiting cases for experimental values are indicated by the horizontal solid lines.

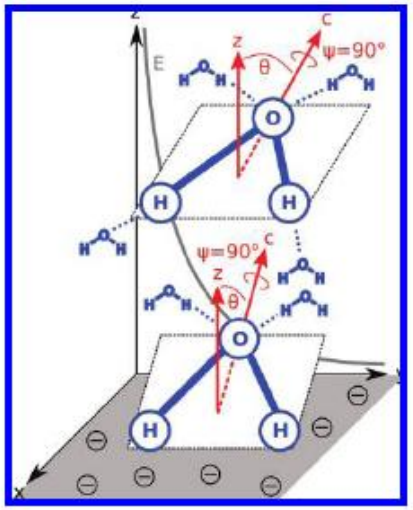

Figure 9. One scenario for water structure at the fused silica interface. Here tetrahedral water molecules are oriented with large tilt angles, some distance from the interface. Close to the interface, molecules with lower H-bonding coordination have smaller tilt angles. Both species have a twist angles of 90°, so the H−O−H plane is approximately parallel to the plane of the interface.

Results

2. Water Orientation at the Fused Silica Surface

Case 2: Tetrahedral Species in the Plane of the Interface, Lower Coordination Species Perpendicular to This Plane

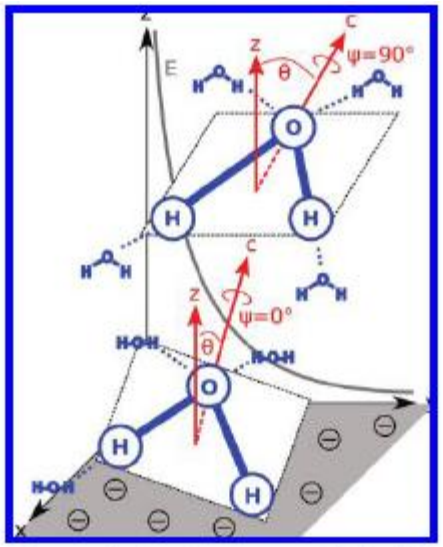

Figure 10. One scenario for water structure at the fused silica interface. Here tetrahedral water molecules are oriented with large tilt angles and twist angles close to 90°, some distance from the interface. Close to the interface, molecules with lower H-bonding coordination have smaller tilt angles and a twist angle of 0°.

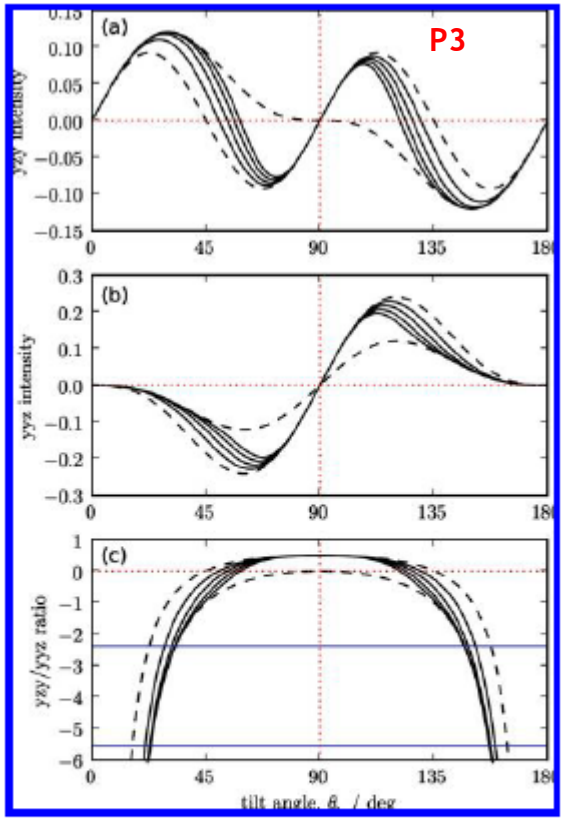

Figure 11. Prediction of (a) A_{yzy} and (b) A_{yyz} amplitude as a function of the mean tilt angle for the P_3 population antisymmetric stretch with our hybrid orientation distribution function. Here, in the narrow limit, the twist angle is centered at 0° when the water molecules are constrained by large tilt angles. For comparison, the limiting cases of wide/uniform and fixed twist angles are shown with dashed lines. (c) The A_{yzy}/A_{yyz} ratio. Limiting cases for experimental values are indicated by the horizontal solid lines.